International Journal of Applied Pharmaceutics

ISSN- 0975-7058 Vol 18, Issue 1, 2026

Original Article

GASTRO-RETENTIVE SUSTAINED RELEASE MUPS (MULTI-UNIT PARTICULATE SYSTEM) OF RIVAROXABAN FOR ORAL ADMINISTRATION

PRAVEEN KUMAR S. VERMA, PRAKASH K. SONI*, REENA SONI, SURESH K. PASWAN

Nanotechnology Research Lab, Department of Pharmacy, Shri G. S. Institute of Technology and Science, 23-Park Road, Indore-452003 (M. P.), India

***Corresponding author: Prakash K. Soni; *Email: soniprakashpharma@gmail.com**

Received: 22 Jul 2025, Revised and Accepted: 28 Oct 2025

ABSTRACT

Objective: This study focuses on the development and evaluation of gastro-retentive multi-unit particulate systems (MUPS) by utilizing fluidized bed coater, for the oral delivery of rivaroxaban, a direct oral anticoagulant (DOAC).

Methods: The method involves coating of three layers comprising the drug layer, effervescent layer, and polymer layer, each layer containing specific ingredients. These solutions were magnetically stirred, filtered, and coated onto sugar spheres (sucrose) using a Fluidized bed coater (FBC) (P+AM Glatt). The coated pellets were evaluated for parameters like particle size, friability, buoyancy, *in vitro* drug release, swelling studies differential scanning calorimetry (DSC) analysis, scanning electron microscopy (SEM), and capsule filling performance. The method is designed in order to optimize the coating process and to assess the quality of pellets and enhance the drug delivery of rivaroxaban.

Results: Batch N-IV (4% Eudragit NM 30D) achieved 84.8% sustained drug release over 24 h with minimal burst (20.85% at 1 h), fitting the Korsmeyer-Peppas model (R^2=0.995, n=0.647). This formulation floated rapidly (2.15 min lag time) for>24 h, and exhibited excellent physical properties (friability: less than 1%; Carr's index: 0.842%; Hausner ratio: 1.008), with high drug loading (17.11 mg/250 mg pellets), and high coating efficiency (98.6%).

Conclusion: Compared to immediate-release formulations, the MUPS-based approach improved gastric retention, provide sustain release and improve dissolution profile along with a reduction in dosing frequency.

Keywords: Rivaroxaban, Gastro-retentive, Sustain release, Fluidized bed coater, Eudragit NM 30D

DOI: https://dx.doi.org/10.22159/ijap.2026v18i1.56204 Journal homepage: https://innovareacademics.in/journals/index.php/ijap

INTRODUCTION

Rivaroxaban (marketed as Xarelto®) is an oral anticoagulant medication utilized to prevent blood clotting. In contrast to traditional blood thinners such as warfarin, which disrupt vitamin K-dependent clotting factors, rivaroxaban directly targets factor Xa, an essential enzyme in the blood coagulation process. Marketed as Xarelto®it only comes in an immediate-release film-coated tablet and oral suspension (for pediatric and patients having swallowing difficulties). Xarelto's absorption is dose-dependent and affected by food with low gastric retention [1-5]. Studies shows that the sustained-release formulation of rivaroxaban displays a higher bioavailability as compared to the marketed formulation Xarelto® [6]. Studies shows that XARELTO should not be released in distal part of the stomach to work properly. If it's released further down in the intestines, absorption will be reduced, and the drug will be less effective [7-10].

The immediate release dosage form of rivaroxaban suffers from the drawback of needing of frequent dosing (poor compliance), sharp plasma peaks (increased bleeding risk) and, low bioavailability of higher doses due to poor solubility and short retention in gastric media [11].

Gastro-retentive drug delivery system (GRDDS) system stays long in the gastric media, where the drug is released slowly and the maximum drug absorption is facilitated from the absorption window [12]. The release of medication can be sustained by developing various kinds of GRDDS [13-17]. GRDDS are ideal for drugs requiring absorption in the stomach (e. g., rivaroxaban), pH-sensitive degradation (e. g., antacids), or for drugs having short absorption windows (e. g., vitamins) [15]. They enhance bioavailability, reduce dosing frequency, prevent rapid metabolism, and enable sustained release, improving treatment efficacy and patient compliance. GRDDS include various types which are designed to prolong gastric residence time: floating systems that levitate on gastric fluid, mucoadhesive systems that stick to the stomach lining, expandable systems that swell to resist gastric emptying, high-density systems that sink and remain stationary and magnetic systems retained by external magnetic fields. Each type ensures sustained drug release by delaying transit through the stomach [13, 18]. Various factors affect the retention of medication in the stomach. Age and gender play significant roles in gastric retention time. Interestingly, women tend to have slower stomach emptying rates than men, regardless of differences in body size or weight. Additionally, gastric retention increases with age, individuals over 70 years of age experience longer gastric retention time compared to younger adults. In contrast, newborns show much faster gastric emptying than elderly populations [19-21].

Fluidized bed coater is utilized for coating various formulations to deliver uniform coating, modified drug release, higher coating efficiency, low dust generation, and flexibility. By suspending particles in an air stream, it ensures complete, even coating without agglomeration, while minimizing waste and maximizing yield. Major advantage of utilizing FBC is that it can develop a formulation in which technology transfer can be done with less effort, making it suitable for product development [22-29].

There are various core materials, including powder, pellets, granules, etc. Modern pharmaceutical pellet technology utilizes tiny spheres (0.5–2 mm) which are coated to enhance drug delivery, offering formulations such as slow-release pellets for controlled dosing, instant-release pellets for rapid effect, flavor-concealing pellets to improve taste, and stomach-retaining pellets for targeted absorption, all designed to optimize drug efficacy, patient compliance, and therapeutic outcomes [30, 31].

The purpose of this study was to develop MUPS-based gastro-retentive formulation of rivaroxaban using FBC technique, with an objective to achieve long gastric retention, to sustain the release of drug for 24 h, to decrease the dosing frequency of rivaroxaban, and improve dissolution profile of the same. MUPS by nature spread evenly throughout the stomach and upper small intestine. This leads

to a more consistent and predictable rate of drug absorption compared to a single monolithic tablet like Xarelto®. To verify that the coating process is optimal and controlled, coating was applied on the core, various parameters like drug loading, process efficiency, micromeritic properties, particle size distribution and, dissolution studies were performed [32-34]. After analyzing the given parameters, the optimized batch was then evaluated for drug release kinetics, SEM and DSC, after which filling of coated pellets into capsules was done.

MATERIALS AND METHODS

Materials

Rivaroxaban was provided by Dr. Reddy's laboratories Ltd. Telangana (India), sugar beads were provided by JRS pharma Nandasan, (India), Eudragit NM 30D was procured from Evonik (Germany), Hydroxypropyl Methylcellulose E50 and E15 (HPMC E50 and HPMC E15) were provided by Colorcon Goa (India). Polyethylene Glycol 6000 (PEG 6000), triacetin, and sodium bicarbonate were received from Loba Chemie Pvt. Ltd. Mumbai, (India), and tween 80 was purchased from Merck life science Pvt. Ltd. Mumbai, (India). The solvents used in this experiment were purchased from S D Fine-Chem Limited Mumbai, (India). The chemicals and solvents used during this work were of pure and analytical grade.

Methods

Preparation of coating solution for drug layering

The coating solution was prepared by dissolving HPMC E50 in mixture of isopropyl alcohol (IPA) and dichloromethane (DCM) in a 3:7 ratio under magnetic stirring at 1200 revolutions per minute (RPM) for 5 min to form a clear solution. PEG 6000 was then added and stirred for an additional 5 min to ensure homogeneity. Next, rivaroxaban, was incorporated into the mixture and mixed for 10 min until a complete dispersion was achieved. Tartrazine yellow was subsequently added, followed by another 5 min of stirring to ensure uniform distribution. The final solution was filtered through an American Society for Testing and Materials (ASTM) #100 mesh sieve to remove any undissolved particles. To prevent the solution from evaporating, the beaker was covered in aluminum foil and continuously stirred using a magnetic stirrer to maintain consistency. The entire preparation was carried out under controlled conditions to maintain uniformity [35]. The composition of the drug layering solution is mentioned in table 1.

Table 1: Composition of drug layering solution

S. No.	Ingredients	Function	Percentage	Quantity
1.	Rivaroxaban	Drug	8%	4 gm
2.	HPMC E50	Binder	0.8%	400 mg
3.	PEG 6000	Plasticizer	0.5%	250 mg
4.	Tartrazine yellow	Colorant	0.1%	50 mg
5.	IPA: DCM (3:7)	Solvent (q. s.)	100%	50 ml

Preparation of coating solution for effervescent layering

The effervescent layering solution was prepared by dissolving HPMC E50 in a solvent blend of IPA and DCM in a 7:3 ratio under continuous stirring until a clear solution was obtained. Sodium bicarbonate was then dispersed into the mixture and stirred for 30 min to ensure uniform distribution. Triacetin was subsequently added to enhance film flexibility and adhesion. The resulting solution was filtered through an ASTM #100 mesh sieve to remove any undissolved particles, ensuring a smooth and homogeneous consistency. To prevent evaporation of solvent, the solution was protected by covering the beaker with aluminum foil. Throughout the entire process, continuous stirring was maintained using a magnetic stirrer to prevent sedimentation and ensure uniformity. This method produced a stable and well-dispersed effervescent layering solution suitable for effervescent coating. The composition of the effervescent layering solution is mentioned in table 2.

Table 2: Composition of effervescent layering solution

S. No.	Ingredients	Function	Quantity	
			B Ⅰ	B Ⅱ*
1.	Sodium bicarbonate	Effervescent agent	2 gm	2 gm
2.	HPMC E50	Binder	400 mg	500 mg
3.	Triacetin	Plasticizer	250 mg	250 mg
4.	IPA: DCM (7:3)	Solvent (q. s.)	50 ml	50 ml

*Represents optimal formulation batch.

Table 3: Composition of polymer coating solution

S. No.	Ingredient	Function	Quantity in different batches					
			N- Ⅰ	N- Ⅱ	N- Ⅲ	N- Ⅳ	N- Ⅴ	N- Ⅵ
1.	Eudragit NM 30D	Sustain release polymer (ml)	0.5	1	1.5	2	2.5	5
2.	HPMC E15	Binder (mg)	250	250	250	250	250	250
3.	Tween 80	Plasticizer (mg)	250	250	250	250	250	250
4.	Magnesium stearate	Anti-adherent (mg)	250	250	250	250	250	250
5.	Talc	Anti-tacking agent (mg)	500	500	500	500	500	500
6.	Sunset yellow	Colorant (mg)	100	100	100	100	100	100
7.	IPA: DCM (7:3)	Solvent (ml) (q. s.)	50	50	50	50	50	50

Preparation of coating solution for polymer layering

The coating solution was prepared by first adding Eudragit NM 30D into a beaker, followed by the incorporation of sunset yellow dye as a colorant. IPA was then introduced and mixed under magnetic stirring at 1200 rpm for 5 min to achieve a clear, homogeneous mixture. DCM was subsequently added to adjust the solubility of HPMC E15 prior adding it into the solution. Next, tween 80 (a surfactant) and talc (an anti-tacking agent) were added, and the mixture was stirred for an additional 10 min to ensure complete

dissolution of all components except talc, which remained suspended. The final solution was filtered through an ASTM #100 mesh sieve to remove any undissolved particles, ensuring a smooth and uniform coating suspension. To prevent evaporation of solvent, the solution was protected by covering the beaker with aluminum foil. Throughout the process, continuous stirring was maintained to prevent sedimentation and addition of magnesium stearate was done in the interval of 60 min to prevent adhesion of coated pellets with the surroundings. The composition of the polymer layering solution is mentioned in table 3.

Process optimization

The air suspension coating process was optimized across three critical stages: drug layering, effervescent layering, and polymer coat layering, to ensure uniform coating deposition and optimal product performance. Sugar pellets (sucrose) were selected as the core material for coating as they have an optimal size (600 µm) and their inherent mass requires the effervescent layer to generate sufficient gas volume (dictated by its thickness/composition) to achieve the critical density reduction (<1.0 g/cm^3) necessary for reliable buoyancy.

For drug layering, the process was started with system preheating at 35 °C, using an initial fluidization pressure of 0.09 MPa and atomization pressure of 0.65 MPa to establish stable bed fluidization. The spray rate was gradually increased from 0.3 to 0.5 rpm while adjusting fluidization pressure (0.09-0.11 MPa) and an atomization pressure (0.7-1.2 MPa) over a 130 min period. This incremental optimization prevented over-wetting while ensuring homogeneous drug distribution. The stage concluded with controlled drying to stabilize the drug-loaded cores before subsequent layering.

Effervescent layering was employed using a modified parameter which, was set to accommodate the unique properties of effervescent components. While maintaining the same temperature profile (35 °C inlet), higher atomization pressures (0.8-1.3 MPa) were used to achieve finer droplet formation. Fluidization pressure was also elevated (0.11-0.13 MPa) to maintain adequate particle mobility and prevent agglomeration. These adjustments were critical in preserving the effervescent functionality while achieving a defect-free layer.

The final polymer coating was implemented to sustain the drug release. Using standardized conditions across all batches (N- I to N-Ⅵ),with strict control over inlet temperature (35 °C) and product temperature (33-34 °C). Spray rates were maintained between 0.1-0.5 rpm, while fluidization (0.09-0.15 MPa) and atomization pressures (0.8-1.8 MPa) were scaled according to polymer concentration. Addition of magnesium stearate was done every 60 min to prevent sticking of pellets. This flexibility ensured optimal film formation across different formulations while maintaining coating integrity.

Process efficiency

The process efficiency of Eudragit NM 30D-coated pellets was determined on the basis of the theoretical yield and the practical yield of coated pellets.

$$\%\text{Process efficiency} = \frac{\text{Practical Yield}}{\text{Theoretical Yield}} \times 100$$

Theoretical and practical yields along with process efficiency of all formulated batches are shown in table 4.

Table 4: Theoretical and practical yields of all batches and their process efficiency

S. No.	Formulation batch	Yield (gm)		Weight loss after sieving (mg)	Process efficiency (%)
		Theoretical yield	Practical yield		
1.	N- Ⅰ (1%)	55.45	55.34	110	99.80
2.	N- Ⅱ (2%)	55.60	55.10	500	99.10
3.	N-Ⅲ (3%)	55.75	54.95	800	98.56
4.	N-Ⅳ (4%)	55.90	55.12	780	98.60
5.	N- Ⅴ (5%)	56.05	55.35	700	98.75
6.	N-Ⅵ (10%)	56.80	55.57	1230	97.83

Drug loading

To determine drug loading on the primary layer, 250 mg of layered pellets were dissolved in 500 ml of acetate buffer (pH 4.5)+0.5% SLS and mixed for 1 h. 1 ml of this solution was diluted 10 times and filtered in order to analyze it on a UV spectrophotometer (Shimadzu 1700), and the concentration was found to be 3.774 gm for 50 gm and 18.87 mg for a dose of 250 mg.

The process efficiency in the drug layering stage was calculated using the formula:

$$\%\text{ Coating efficiency} = \frac{\text{Practical yield}}{\text{Theoretical yield}} \times 100$$

Where,

Practical yield = 53.2 g

Theoretical yield = 54.7 g

The process efficiency in the drug layering stage was found to be 97.25%.

Drug loading of Eudragit NM30D-coated pellets was determined by dividing the theoretical amount of drug by the total weight of pellets after polymer coating. Further dividing the value by four gives the concentration of the drug present in a dose of 250 mg.

$$\text{Drug loading per 250 mg} = \frac{\text{Total drug in mg}}{\text{Total weight gain of pellets after polymer layer coating} * 4}$$

#Total drug = 3774 mg

Drug loading in all batches is summarized in table 5.

Evaluation of prepared MUPS

Particle size distribution

Sieve analysis was performed to determine the size of coated MUPS. 50 gm of the coated pellets were weighed and then transferred onto a stacked series of sieves. A mechanical shaker (Retsch AS-200) was then used to shake these sieves for 10 min at an amplitude of 50. Following shaking, each sieve's retained pellets were weighed independently [36, 37].

Table 5: Drug loading of eudragit NM 30D-coated pellets

S. No.	Formulation batch	Practical yield (gm)	Drug loading of coated pellets (per 250 mg)
1.	N- Ⅰ (1%)	55.34	17.04 mg
2.	N- Ⅱ (2%)	55.10	17.12 mg
3.	N-Ⅲ (3%)	54.95	17.17 mg
4.	N-Ⅳ (4%)	55.12	17.11 mg
5.	N- Ⅴ (5%)	55.35	17.04 mg
6.	N-Ⅵ (10%)	55.57	16.97 mg

Friability

The friability of Eudragit NM 30D-coated pellets was evaluated using FBC and Roche friabilator apparatus. For determining friability in FBC, 50 gm of coated pellets were suspended in a Wurster chamber for 30 min under specific parameters (0.40 bar fluidizing air pressure, 1.20 bar atomization air pressure, and 35 °C inlet air temperature). For Roche friability testing, 10 gm of coated pellets were tumbled in a friabilator at 25 rpm for 100 revolutions, then sieved through an ASTM #24 mesh sieve [37-39]. Pellets generally tolerate higher friability than tablets due to their larger surface area and processing dynamics.

The percentage friability (%F) was calculated as:

$$F\% = [\frac{(W^0 - Wt)}{W^0}] \times 100$$

where W_0 is the initial pellet weight and W_t is the weight retained after sieving.

Micromeritics properties (tapped and bulk density)

To assess pellet micromeritics properties, bulk density was determined by weighing 50 gm of Eudragit NM 30D-coated pellets and then transferring them into a 100 ml measuring cylinder, and bulk density was calculated as weight divided by settled volume. Tapped density was measured using United States Pharmacopeia (USP) II method with an Electrolab ETD 1020x tester, where the same sample was tapped, and the volume recorded, with tapped density calculated as weight over tapped volume. From these values, Carr's compressibility index and Hausner ratio were derived to evaluate flowability, which helps assess pellet characteristics such as cohesiveness, particle size, and surface properties [40-42].

$$\text{Carr's Index} = [\frac{(\text{Tapped density} - \text{Bulk density})}{\text{Tapped density}}] \times 100$$

and,

Hausner ratio = Tapped density/Bulk density

Buoyancy (floating lag time and floating time)

The buoyancy behavior of Eudragit NM 30D-coated pellets was evaluated using USP type II dissolution apparatus (Electrolab) with acetate buffer (pH 4.5) and 0.5% SLS at 75 rpm [43].

***In vitro* drug release (using USP type 2 paddle apparatus)**

The drug release study of coated pellets (n=3) was performed using a USP Type II dissolution apparatus (Electrolab) with 900 ml of acetate buffer (pH 4.5) and 0.5% SLS as the medium, maintained at 37±0.5 °C with 75 rpm agitation. The acetate buffer (pH 4.5) and 0.5% SLS was selected as a dissolution media to dissolve a sufficient amount of rivaroxaban and to maintain the sink conditions [44]. The 24 h test compared sustained-release pellets (250 mg samples) from experimental batches against the commercial product Xarelto®, with 10 ml samples collected at scheduled intervals and replaced with fresh medium to maintain sink conditions. Rivaroxaban release was quantified using UV spectrophotometry (Shimadzu 1700) at 248 nm [45].

Drug release kinetics

To elaborate on how rivaroxaban is released from Eudragit NM 30D-coated pellets, the in vitro release data were assessed by utilizing multiple release models to identify the fundamental process of medication discharge. This included five kinetic models: zero-order, first-order, Hixson-Crowell, Korsmeyer-Peppas, Weibull, and Higuchi [46-49].

Swelling studies

The swelling behavior of the coated pellets was investigated using light microscopy to provide a direct visual assessment of the film's performance in a physiologically relevant environment. For this analysis, individual pellets were mounted on a grooved glass slide, and a drop of 0.1N HCl was introduced to simulate the acidic conditions of the stomach. This setup allowed for the real-time observation of critical phenomena such as the initiation of swelling, the rate of fluid penetration, the physical expansion of the pellet core, and the integrity and potential rupture of the functional coating as it interacted with the acidic medium.

Scanning electron microscopy (SEM) and cross-sectional light microscopy

A small quantity of layered pellets was placed on an aluminum pin stub with the help of carbon conductive double-faced adhesive tape, and morphological images of the pellets were observed under a field emission scanning electron microscope (FE-SEM). The scanning electron microscopy of 4% Eudragit NM 30D-coated pellets was performed using Zeiss Gemini SEM 360 [50]. A light microscopy was also performed using light microscope for the cross-sectional view of coated pellet.

Differential scanning calorimetric analysis (DSC)

The thermal analysis of Eudragit NM 30D-coated MUPS, sugar beads, sodium bicarbonate, HPMC, PEG 6000, rivaroxaban and their physical mixture (sugar beads+sodium bicarbonate+HPMC+PEG 6000+rivaroxaban) was performed using a differential scanning calorimeter (Perkin Elmer 6000, Waltham, MA, USA). Approximately 3 mg samples were weighed, then sealed in an aluminum pan, and it was then placed in the sample holder; likewise, a blank aluminum pan was also placed as a reference. Then it was further heated at a temperature range of 50 °C to 300 °C at a rate of 40 °C/min in a nitrogen environment [51-53]. The thermograms were recorded between 50 °C and 300 °C taking empty aluminum pan as reference [54].

Filling of coated pellets into capsules

The selection of a suitable capsule was done on the basis of their capacity to hold a specific quantity of pellets. The capsules were loaded manually, which involved dividing the cap and base of each empty capsule. Disintegration test of selected capsules was performed using disintegration test apparatus (Electrolab USP ED 2L), and *in vitro* drug release from capsules (n=3) was determined using USP Type II dissolution apparatus (Electrolab) [55-57].

RESULTS AND DISCUSSION

Particle size distribution

The size distribution of uncoated core particles (plane spheres) and Eudragit NM 30D coated pellets is summarized in table 6 and shown in fig. 1. Uncoated cores ranged between 600-850 µm in diameter, while all coated pellets exceeded 850 µm, confirming that the coating process significantly increases particle size.

The results demonstrate a direct relationship between coating concentration and pellet growth, which implies that increasing the Eudragit NM 30D concentration will result in proportionally thicker layers and larger final pellet diameters.

Importantly, the Eudragit NM 30D coated pellets showed minimal size variation, indicating excellent process control and uniformity. This narrow size distribution suggests highly consistent coating thickness across all formulations.

Table 6: Sieve analysis of core pellets and Eudragit NM 30D coated pellets of rivaroxaban

S. No.	Sieve no. (passed/retained)	Pore size (µm)	% Weight retained*						
			Plain sphere	N- Ⅰ	N- Ⅱ	N-Ⅲ	N-Ⅳ	N- Ⅴ	N-Ⅵ
1.	Above 20	More than 850	10.2±0.98	90.27±2.97	91.43±1.05	92.23±1.35	92.87±0.43	93.25±0.74	96.42±1.34
2.	20/30	600-850	89.89±1.29	9.23±1.10	8.2±0.35	6.76±0.08	6.22±0.19	5.31±0.08	3.92±0.67
3.	30/40	425-600	-	-	-	-	-	-	-
4.	40/60	250-425	-	-	-	-	-	-	-
5.	60/80	180-250	-	-	-	-	-	-	-
6.	80/100	150-180	-	-	-	-	-	-	-

*Data presented as mean ±SD (n=3)

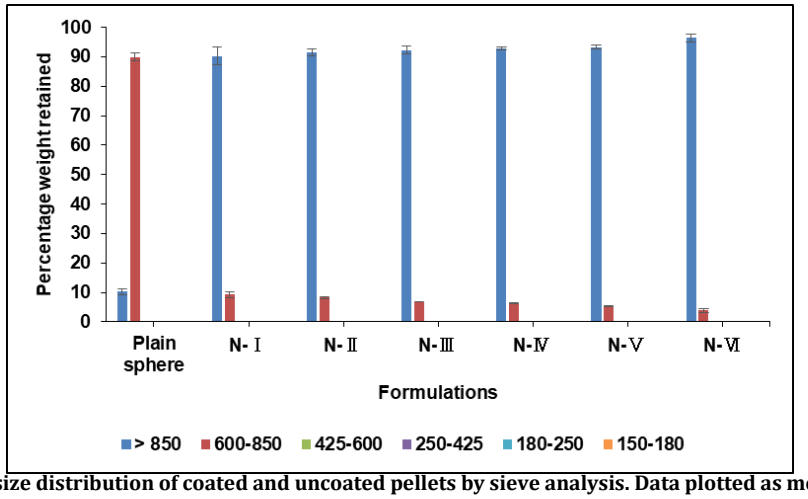

Fig. 1: Particle size distribution of coated and uncoated pellets by sieve analysis. Data plotted as mean ±SD (n=3)

Friability

The friability of coated pellets was evaluated across six batches (N-I to N-VI, representing 1%, 2%, 3%, 4%, 5% and 10% polymer coating) using both a fluidized bed coater (FBC) and a Roche friabilator apparatus and noted in table 7. Excellent mechanical resistance was demonstrated by all batches, with percentage friability values consistently recorded between 0.13% under both test conditions. These values were observed to be significantly below the standard acceptance criterion of 1.0% of tablets as well as pellets [58].

Furthermore, the friability values obtained under the FBC method were determined to be highly comparable to those measured under the traditional Roche friabilator, indicating no significant difference between the two testing methodologies. The minimal friability was consistently exhibited across all coating levels and in both test apparatuses, confirming high product integrity.

Table 7: Friability of Eudragit NM 30D coated pellets

S. No.	Formulation batches	Percentage friability	
		Under FBC	Under roche friabilator
1.	N-Ⅰ (1%)	0.11	0.10
2.	N-Ⅱ (2%)	0.13	0.13
3.	N-Ⅲ (3%)	0.11	0.10
4.	N-Ⅳ (4%)	0.13	0.12
5.	N-Ⅴ (5%)	0.11	0.13
6.	N-Ⅵ (10%)	0.10	0.12

Micromeritics properties (tapped and bulk density)

The effect of increasing polymer coating levels on pellet flow properties was assessed and noted in table 8. A progressive increase in bulk density (from 0.817 to 0.868 g/cc) and tapped density (from 0.821 to 0.879 g/cc) was observed with increasing Eudragit NM 30D coating percentages. Consequently, the compressibility index was also increased from 0.49% to 1.2%, and the Hausner ratio was increased from 1.004 to 1.012. However, all Carr's compressibility index values were maintained well below 10%, and all Hausner ratios were kept less than 1.11. Excellent flow characteristics were consistently demonstrated across all batches, indicating that the increased coating did not compromise pellet handling properties.

Table 8: Micromeritics properties of coated pellets

S. No.	Formulation code	Parameter			
		Bulk density (g/cc)	Tapped density (g/cc)	Carr's index (%)	Hausner ratio
1.	N-Ⅰ (1%)	0.817	0.821	0.49	1.004
2.	N-Ⅱ (2%)	0.818	0.823	0.607	1.006
3.	N-Ⅲ (3%)	0.822	0.828	0.72	1.007
4.	N-Ⅳ (4%)	0.824	0.831	0.842	1.008
5.	N-Ⅴ (5%)	0.830	0.839	1.07	1.010
6.	N-Ⅵ (10%)	0.868	0.879	1.2	1.012

Table 9: Buoyancy study of developed pellets

S. No.	Formulation code	Floating lag time (min)
1.	N-Ⅰ (1%)	1.14
2.	N-Ⅱ (2%)	1.32
3.	N-Ⅲ (3%)	1.54
4.	N-Ⅳ (4%)	2.15
5.	N-Ⅴ (5%)	3.28
6.	N-Ⅵ (10%)	7.23

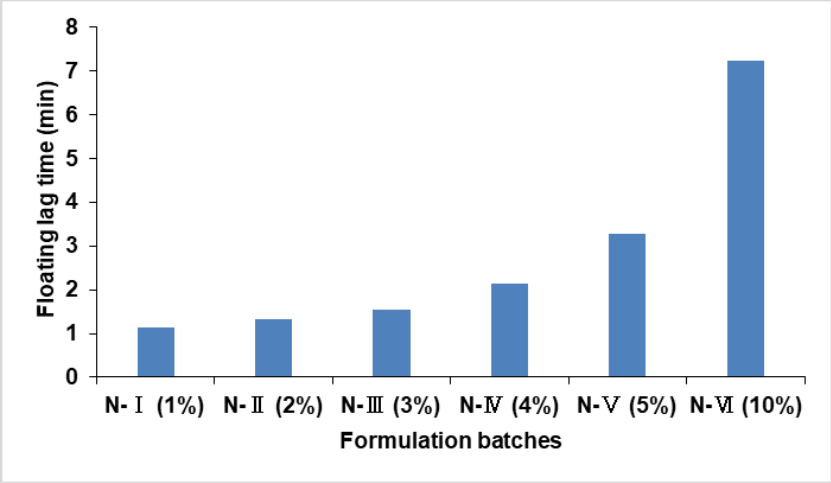

Fig. 2: Floating lag time of N-Ⅰ (1%), N-Ⅱ (2%), N-Ⅲ (3%), N-Ⅳ (4%), N-Ⅴ (5%), and N-Ⅵ (10%) Eudragit NM 30D coated pellets

Buoyancy (floating lag time and floating time)

Buoyancy study of all batches are mentioned in table 9 and represented in fig. 2. Study displays that floating lag time increases as the polymer (Eudragit N30 D) concentration increases. The floating time of coated pellets was seen for 24 h; all the coated pellets (100%) were seen floating except pellets coated with 1% Eudragit NM 30 D.

***In vitro* drug release (using USP type 2 paddle apparatus)**

In vitro drug release was performed and results are shown in table 10 and graphically presented in fig. 3. The release of N-Ⅰ (1% Eudragit NM 30D coated pellets) shows a burst release along with minimal floating time of pellets, while the other formulations N-Ⅱ (2% Eudragit NM 30D coated pellets), N-Ⅲ (3% Eudragit NM 30D coated pellets) and N-Ⅵ (4% Eudragit NM 30D coated pellets) show a sustained release over 24 h. All batches were seen floating above the dissolution media for 24 h, except batch N-Ⅰ. Formulations N-Ⅴ and N-Ⅵ show a sustained release (>80% drug release) for 30 and 48 h, respectively.

This indicates that the percentage drug release of prepared formulations is directly proportional to the concentration of the polymer (Eudragit NM 30D), which implies that the erosion of Eudragit NM 30D is pH independent and can sustain the drug release over a prolonged time period.

Table 10: *In vitro* drug release data of different batches of Eudragit NM 30D-coated pellets

S. No.	Time (h)	% Cumulative drug release*						Marketed product
		N-Ⅰ (1%)	N-Ⅱ (2%)	N-Ⅲ (3%)	N-Ⅳ (4%)	N-Ⅴ (5%)	N-Ⅵ (10%)	
1.	1	66.63±3.62	31.43±6.17	29.09±3.13	20.85±3.60	17.66±1.94	3.34±1.28	99.88±0.41
2.	2	73.27±4.00	44.32±6.63	38.49±4.11	31.43±3.00	23.57±4.77	7.12±1.33	99.11±0.57
3.	4	79.32±3.75	54.08±5.70	50.25±3.99	42.48±3.24	29.08±3.38	11.41±1.78	99.27±0.04
4.	6	81.25±2.22	59.50±1.14	55.20±1.09	48.50±0.86	34.90±1.53	15.70±0.66	99.31±0.02
5.	8	83.18±4.78	64.60±4.67	58.69±4.55	53.53±1.26	39.69±3.79	18.65±1.49	97.52±0.85
6.	12	98.95±0.66	98.45±1.35	71.30±0.74	63.83±2.15	46.82±1.28	24.34±1.71	97.43±0.27
7.	24	99.63±0.28	98.26±1.38	92.90±2.90	84.80±2.15	55.29±4.61	33.00±3.63	96.51±0.52

*Data presented as mean ±SD (n=3)

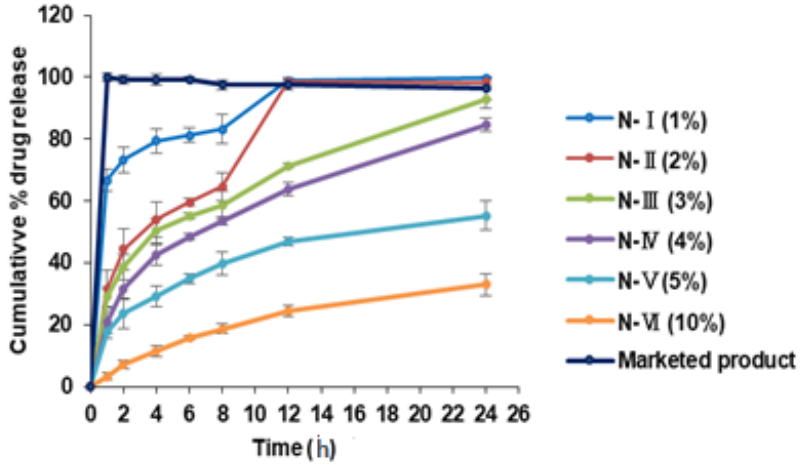

Fig. 3: *In vitro* drug release profile of different batches of Eudragit NM 30D-coated pellets of rivaroxaban. Data plotted as mean±SD; (n=3)

Swelling studies

The swelling studies were performed using light microscopy and the results are shown in fig. 4. The images were taken at different time points with A at 10 s, B at 30 s, and C at 1 min. The image clearly shows the swelling nature of Eudragit NM 30D and HPMC when they come into contact with gastric media i.e. 0.1 N hydrochloric acid.

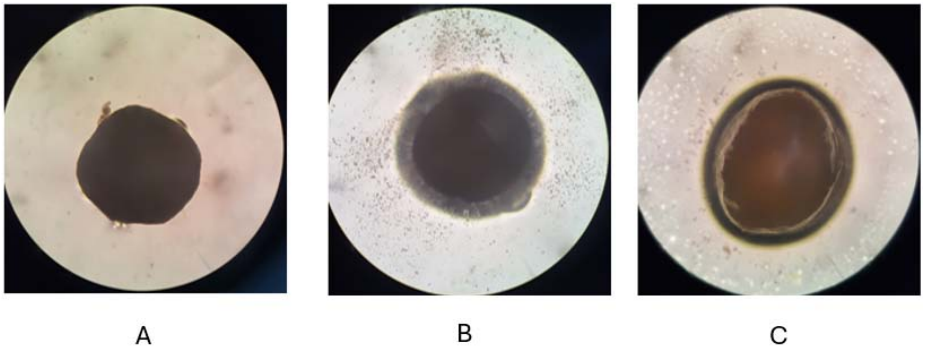

Fig. 4: Observation swelling studies of 4 % Eudragit NM 30D coated pellets

Scanning electron microscopy (SEM) and cross-sectional light microscopy

Scanning electron microscopy (SEM) of Eudragit NM30D-coated pellets, processed via fluidized bed coater, was performed at 5.00 kV accelerating voltage and 9.0 mm working distance. A uniform, smooth polymeric film was observed across pellet surfaces at both 42X and 79X magnifications using secondary electron (SE2) detection.

The SEM images are shown in fig. 5a, confirming that the pellets were evenly coated and the surface of the layered pellets is mostly smooth with no sign of aggregation. The layered pellets are evenly coated and have a size of above 850 µm. A surface without defects such as cracks, pores, or agglomeration was seen, confirming effective film formation. The integrity of the coating layer was verified, supporting successful atomization and drying during processing. Consistent film quality across samples was evidenced by standardized analytical conditions and defect-free surfaces.

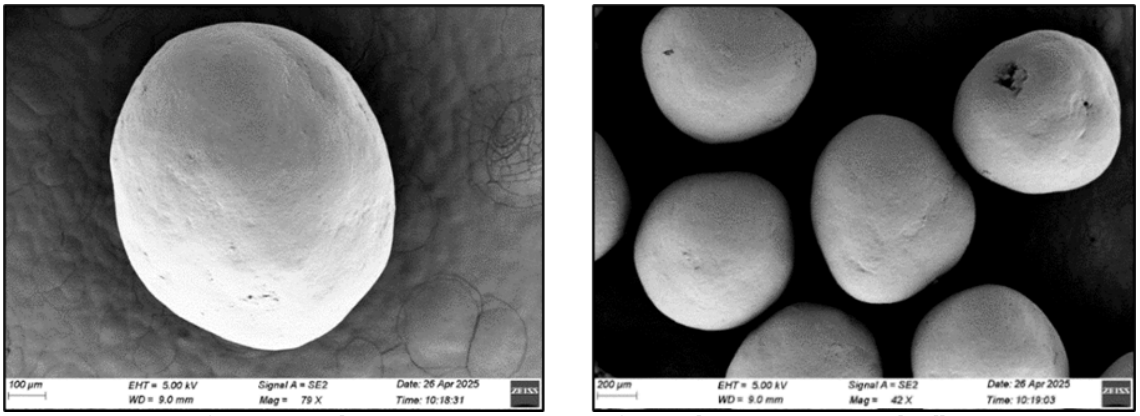

Fig. 5a: Scanning electron microscopic image of 4% Eudragit NM 30D-coated pellets

Fig. 5b: Cross-sectional light microscopy

Drug release kinetic

The kinetics of coated pellets (4% Eudragit NM 30D coated pellets) of rivaroxaban was analyzed with different kinetic models are displayed in fig. 6. The different values of R^2 determined by various kinetic models are shown in table 11. The release profile shows the highest compliance for the Korsmeyer-Peppas model of drug release because it is close to the regression equation and shows the highest value of R^2 i.e. 0.995. Furthermore, the value of release exponent 'n' is 0.6476, and it was concluded that the medication N-Ⅳ (4% Eudragit NM 30D coated pellets) follows anomalous (non-fickian) transport (0.45<n<0.89), which means that the release method is both diffusion and polymer breakdown [59]. To understand the release kinetics of this formulation, model fitting was performed on 2% and 3% also, and both of them showed a high compliance for the Korsmeyer-Peppas model for drug release.

Table 11: Drug release kinetic models of batch N-Ⅳ (4% Eudragit NM 30D coating)

S. No.	Drug release kinetic model	Equation	K	R^2
1.	Zero-order	$Q_t = Q_0 + k_0 t$	0.050	0.797
2.	First-order	$\log Q = \log Q_0 - kt/2.303$	0.001	0.978
3.	Hixson-Crowell	$Q_0^{1/3} - Q_t^{1/3} = kt$	0.001	0.939
4.	Korsmeyer-Peppas	$\log Q - \log Q_0 = \log k + n \log t$	1.03	0.995
5.	Higuchi	$Q_0 - Q_t = k\sqrt{t}$	2.221	0.987
6.	Weibull	$\ln[-\ln(1-F)] = \beta \ln(t - Ti) - \beta \ln(\alpha)$	0.001	0.976

Where: Q_0 = Initial drug concentration, Q⍰ = Amount of drug remaining at time t, t= Time, k = Rate constant, F = fractional drug release (Mt/M∞), α = scale parameter (time constant), β = shape parameter (mechanism indicator).

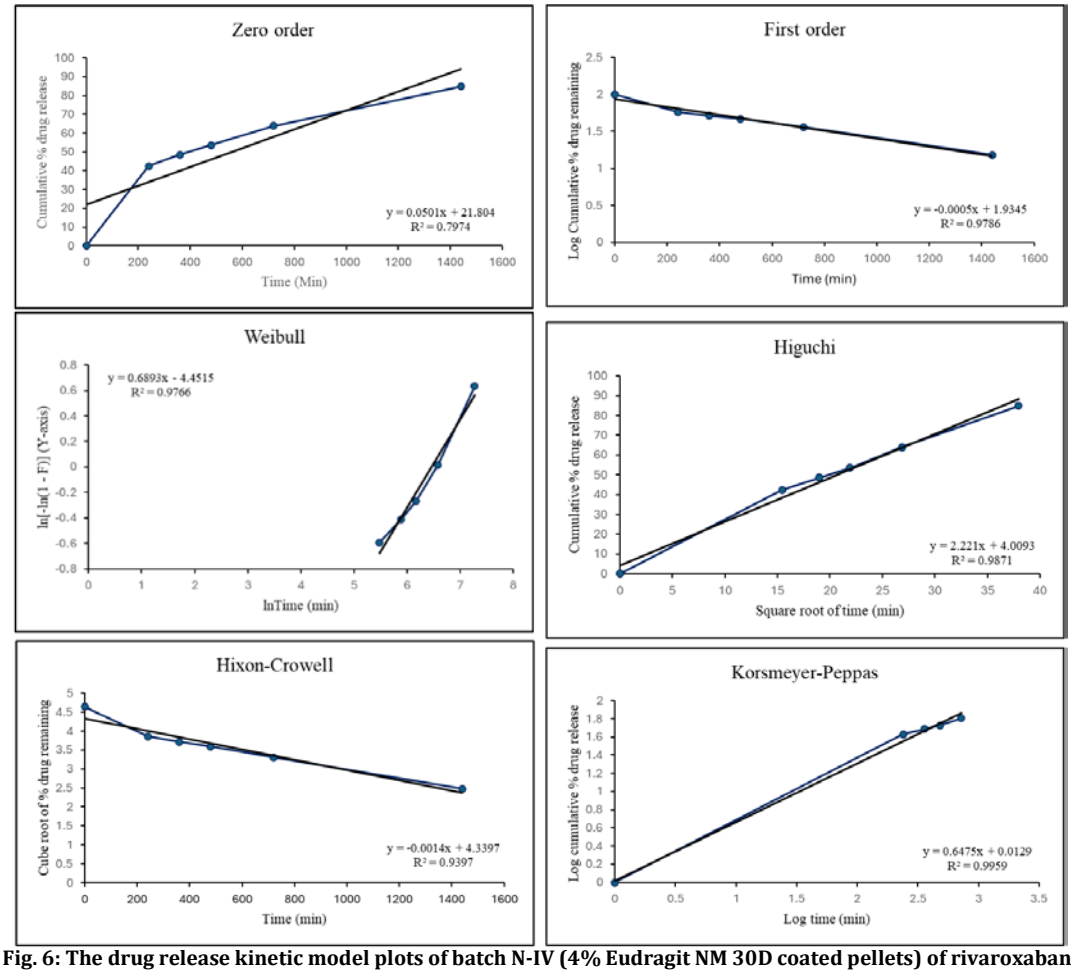

Fig. 6: The drug release kinetic model plots of batch N-IV (4% Eudragit NM 30D coated pellets) of rivaroxaban

Differential scanning calorimetric analysis (DSC)

A DSC thermograph was plotted to characterize the nature of the drugs and excipients, and also to study the drug-excipient interaction. The DSC thermographs of coated MUPS, sugar beads, sodium bicarbonate, HPMC, PEG6000, rivaroxaban and their physical mixture (sugar beads+sodium bicarbonate+HPMC+PEG6000+rivaroxaban) are plotted as shown in fig. 7. An endothermic peak of rivaroxaban at 232.71 °C, sugar beads at 194.37 °C and 251.2 °C, PEG 6000 at 69.25 °C and sodium bicarbonate at 113.15 °C and 161.86 °C confirmed its crystalline nature. The absence of a peak in the HPMC thermograph indicates its amorphous nature. The absence of a peak in the formulation indicates its amorphous nature due to the successful encapsulation of the rivaroxaban. The presence of sharp endothermic peaks of the drug and excipients in the physical mixture depicts no chemical interaction that might lead to any degradation of the formulation. As per the obtained thermogram, it was concluded drug and excipients were pure and free from impurities.

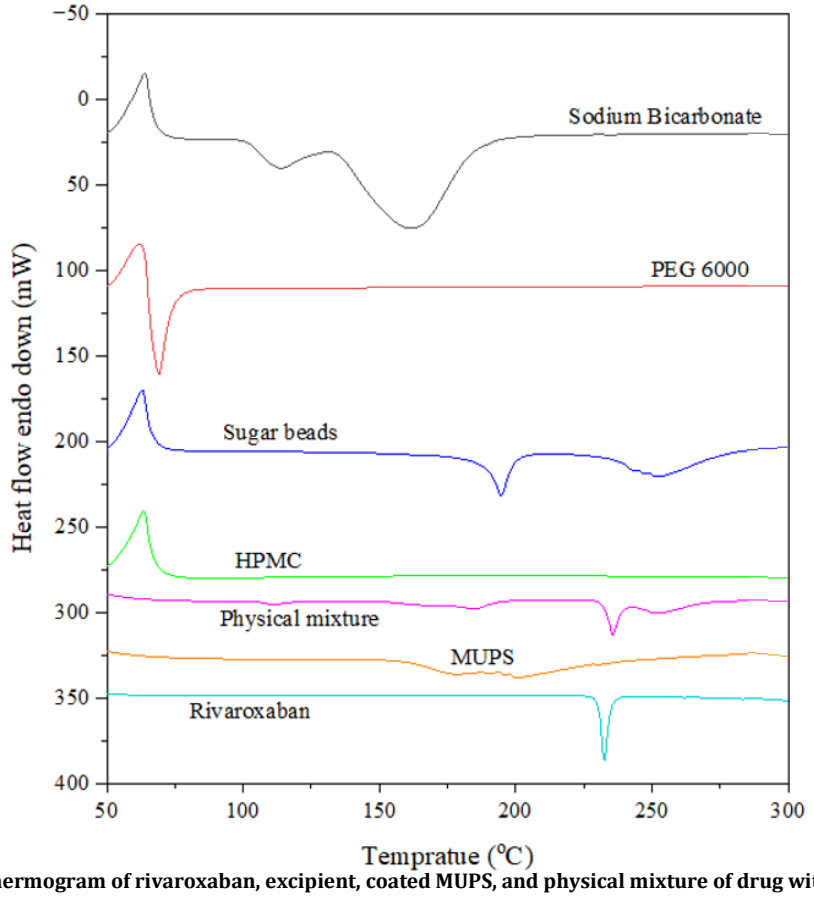

Fig. 7: DSC thermogram of rivaroxaban, excipient, coated MUPS, and physical mixture of drug with excipients

Filling of coated pellets into capsules

Capsule size was selected according to their capacity to hold a certain volume. Size-2 capsules were selected for further processing. Calculation were done on the basis of filling capacity of various capsules along with the quantity of pellets that can be filled in various capsule on the basis of tapped density (0.831 g/cc) of 4 % coated pellets, and are detailed in table 12. It was observed that capsule size 2 accommodated the exact and sufficient quantity of coated pellets required by specifications, with some residual space remaining after filling. The disintegration time of the filled size-2 capsules was determined to be 5 min and 32 s in a 0.1N HCl solution. Furthermore, the *in vitro* release profile of the capsule contents, as presented in table 13 and fig. 8, was found to be identical to that exhibited by 4% Eudragit NM 30 D coated pellets. This confirmed that the desired release characteristics were maintained after encapsulation.

Table 12: Capacity of various capsule according to their size

Capsule size	Filling capacity		Quantity of pellets filled in the capsules (mg)
	mg (for average-density powder)	ml (volume capacity)	
000	700-1,000 mg	1.37	1138
00	500-600 mg	0.90	748
0	300-500 mg	0.68	565
1	200-400 mg	0.48	399
2	150-300 mg	0.36	298
3	100-200 mg	0.27	224
4	75-150 mg	0.20	166
5	50-100 mg	0.13	108

Table 13: *In vitro* drug release data of capsule filled with N-Ⅳbatch

S. No.	Time (h)	Cumulative % drug release			Average cumulative % drug release*
		C1	C2	C3	
1.	1	20.12	21.47	18.14	19.91±1.67
2.	2	31.57	32.86	28.17	30.87±2.42
3.	4	40.58	41.62	35.40	39.20±3.33
4.	8	53.10	55.87	48.24	52.40±3.86
5.	24	85.03	85.97	81.15	84.05±2.55

*Data presented as mean ±SD (n=3)

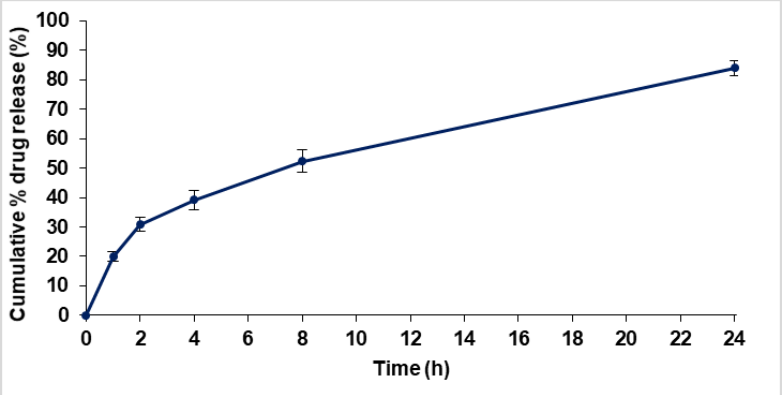

Fig. 8: *In vitro* drug release profile of capsule filled with N-IV batch. Data plotted as mean ±SD (n=3)

DISCUSSION

The successful development of a gastro-retentive multi-unit particulate system (MUPS) for rivaroxaban using fluidized bed coating technology represents a significant advancement over conventional immediate-release formulations. The optimized batch (N-IV, coated with 4% Eudragit NM 30D) demonstrated sustained drug release over 24 h, with only 20.85% release within the first hour, indicating a minimal burst effect. This sustain release profile is critical for rivaroxaban, which requires administration before the distal part of stomach for optimal bioavailability as per the Xarelto FDA label [10]. The release kinetics followed the Korsmeyer-Peppas model (R^2 = 0.995, n = 0.647), suggesting an anomalous (non-Fickian) diffusion mechanism, where drug release is governed by both diffusion through the polymeric matrix and polymer erosion as stated by previous studies [60]. This aligns with the pH-independent erosion properties of Eudragit NM 30D, making it suitable for sustained release in the variable pH environment of the gastrointestinal tract.

The floating behavior of the MUPS was another key achievement. Batch N-IV exhibited a short floating lag time of 2.15 min and maintained buoyancy for over 24 h, ensuring prolonged gastric retention. This is attributable to the effervescent layer, which generates gas upon contact with gastric fluid, reducing the density of the pellets below that of gastric contents. The swelling studies also shows that the polymer Eudragit Nm 30D and HPMC swell in presence of gastric media and the release was sustained by the same. The uniform coating, as confirmed by SEM, showed a smooth, defect-free surface, which is essential for consistent drug release and buoyancy. The excellent micromeritic properties Carr's index of 0.842% and Hausner ratio of 1.008 indicate superior flow characteristics, which are crucial for industrial capsule-filling processes as suggested by studies [40]. The high process efficiency (98.6%) and consistent drug loading (17.11 mg/250 mg pellets) further underscore the performance of the fluidized bed coating process.

Compared to the marketed immediate-release product (Xarelto®), this MUPS formulation offers several advantages: reduced dosing frequency, minimized peak-trough fluctuations, and improved patient compliance. The successful encapsulation into size-2 capsules without altering the release profile confirms the formulation's practicality for oral administration. Moreover, the DSC results confirmed the absence of drug-excipient interactions, ensuring stability and purity.

CONCLUSION

In conclusion, this study successfully developed a novel gastro-retentive multi-unit particulate system (MUPS) for the sustained oral delivery of rivaroxaban using fluidized bed coating technology. The optimized formulation demonstrated excellent sustained release characteristics, effectively prolonging drug delivery over 24 h while minimizing the initial burst release. The system exhibited rapid and prolonged buoyancy, ensuring extended gastric retention crucial for the optimal absorption of rivaroxaban. Comprehensive evaluation confirmed superior physical properties, including high drug loading, excellent coating efficiency, and desirable micromeritic properties for efficient capsule filling. The release kinetics indicated a combination of diffusion and polymer erosion mechanisms. Compared to conventional immediate-release tablets, this MUPS-based approach offers significant therapeutic advantages, including reduced dosing frequency, more stable plasma levels, and potentially improved patient compliance. The successful encapsulation into hard gelatin capsules without altering the release profile further underscores the formulation's practicality. This research establishes gastro-retentive MUPS as a viable and promising strategy to enhance the therapeutic efficacy and patient acceptability of rivaroxaban.

ACKNOWLEDGMENT

The authors are thankful to Dr. Reddy's Labs. Ltd. for providing the gift sample of rivaroxaban, and Indian Institute of Technology (IIT) Indore for SEM study of final optimized MUPS formulation.

FUNDING

Nil

AUTHORS CONTRIBUTIONS

Praveen Kumar S. Verma conducted all experimental work, operated the laboratory machinery, and was responsible for data collection and curation. Dr. Prakash K. Soni conceptualized and supervised the research project, provided critical guidance on the experimental design, and corrected/revised the manuscript. Reena Soni contributed by expert inputs in drug analysis, data validation and manuscript preparation and correction. Dr. Suresh K. Paswan provided technical support in methodology and operation of the fluidized bed coater and manuscript revision.

CONFLICT OF INTERESTS

The authors report no financial or any other conflicts of interest in this work.

REFERENCES

1. Martin KA, Lee CR, Farrell TM, Moll S. Oral anticoagulant use after bariatric surgery: a literature review and clinical guidance. Am J Med. 2017;130(5):517-24. doi: 10.1016/j.amjmed.2016.12.033, PMID 28159600.
2. Ashton V, Kerolus Georgi S, Moore KT. The pharmacology efficacy and safety of rivaroxaban in renally impaired patient populations. J Clin Pharmacol. 2021;61(8):1010-26. doi: 10.1002/jcph.1838, PMID 33599985.
3. Mastenbroek TG, Karel MF, Nagy M, Chayoua W, Korsten EI, Coenen DM. Vascular protective effect of aspirin and rivaroxaban upon endothelial denudation of the mouse carotid artery. Sci Rep. 2020;10(1):19360. doi: 10.1038/s41598-020-76377-8, PMID 33168914.
4. Alalawneh M, Awaisu A, Abdallah I, Elewa H, Danjuma M, Matar KM. Pharmacokinetics of single-dose rivaroxaban under fed

state in obese vs. non-obese subjects: an open-label controlled clinical trial (RIVOBESE-PK). Clin Transl Sci. 2024;17(6):e13853. doi: 10.1111/cts.13853, PMID 38847347.
5. Harder S. Pharmacokinetic and pharmacodynamic evaluation of rivaroxaban: considerations for the treatment of venous thromboembolism. Thromb J. 2014;12(1):22. doi: 10.1186/1477-9560-12-22, PMID 25698904.
6. Anwer MK, Mohammad M, Iqbal M, Ansari MN, Ezzeldin E, Fatima F. Sustained release and enhanced oral bioavailability of rivaroxaban by PLGA nanoparticles with no food effect. J Thromb Thrombolysis. 2020;49(3):404-12. doi: 10.1007/s11239-019-02022-5, PMID 31898270.
7. Puhr HC, Ilhan Mutlu A, Preusser M, Quehenberger P, Kyrle PA, Eichinger S. Absorption of direct oral anticoagulants in cancer patients after gastrectomy. Pharmaceutics. 2022;14(3):662. doi: 10.3390/pharmaceutics14030662, PMID 35336036.
8. Mani H, Kasper A, Lindhoff Last E. Measuring the anticoagulant effects of target-specific oral anticoagulants reasons methods and current limitations. J Thromb Thrombolysis. 2013;36(2):187-94. doi: 10.1007/s11239-013-0907-y, PMID 23512159.
9. Martin KA, Lee CR, Farrell TM, Moll S. Oral anticoagulant use after bariatric surgery: a literature review and clinical guidance. Am J Med. 2017;130(5):517-24. doi: 10.1016/j.amjmed.2016.12.033, PMID 28159600.
10. Food and Drug Administration. Xarelto FDA package insert. Available from: https://www.accessdata.fda.Gov/drugsatfda_docs/label/2016/202439s017lbl.pdf. [Last accessed on 23 Aug 2025].
11. Homayun B, Lin X, Choi HJ. Challenges and recent progress in oral drug delivery systems for biopharmaceuticals. Pharmaceutics. 2019;11(3):129. doi: 10.3390/pharmaceutics11030129, PMID 30893852.
12. Chaturvedi P, Soni PK, Paswan SK. Designing and development of gastroretentive mucoadhesive microspheres of cefixime trihydrate using spray dryer. Int J App Pharm. 2023;15(2):185-93. doi: 10.22159/ijap.2023v15i2.45399.
13. Mandal UK, Chatterjee B, Senjoti FG. Gastro-retentive drug delivery systems and their *in vivo* success: a recent update. Asian J Pharm Sci. 2016;11(5):575-84. doi: 10.1016/j.ajps.2016.04.007.
14. Murphy CS, Pillay V, Choonara YE, Toit Du LC. Gastroretentive drug delivery systems: current developments in novel system design and evaluation. Curr Drug Deliv. 2009;6(5):451-60. doi: 10.2174/156720109789941687, PMID 19751198.
15. Vinchurkar K, Sainy J, Khan MA, Mane S, Mishra DK, Dixit P. Features and facts of a gastroretentive drug delivery system a review. Turk J Pharm Sci. 2022;19(4):476-87. doi: 10.4274/tjps.galenos.2021.44959, PMID 36047602.
16. Badoni A, Ojha A, Gnanarajan G, Kothiyal P. Review on gastro retentive drug delivery system. J Pharm Innov. 2012;1(8):32-42.
17. Tomar A, Upadhyay A, Gupta SK, Kumar S. An overview on gastroretentive drug delivery system: current approaches and advancements. Curr Res Pharm Sci. 2019;9(1):12-6. doi: 10.24092/CRPS.2019.090102.
18. Tripathi J, Thapa P, Maharjan R, Jeong SH. Current state and future perspectives on gastroretentive drug delivery systems. Pharmaceutics. 2019;11(4):193. doi: 10.3390/pharmaceutics11040193, PMID 31010054.
19. Aulton ME, Taylor K. Aulton's pharmaceutics: the design and manufacture of medicines. Elsevier Health Sciences; 2013.
20. Gandhi A, Verma S, Imam SS, Vyas M. A review on techniques for grafting of natural polymers and their applications. Plant Arch. 2019;19(2):972-8.
21. S Chudiwal V. Innovative technologies for gastro-retentive drug delivery systems. GJPPS. 2018;4(5):1-5. doi: 10.19080/GJPPS.2018.04.555650.
22. Wang LK, Heng PW, Liew CV. Classification of annular bed flow patterns and investigation on their influence on the bottom spray fluid bed coating process. Pharm Res. 2010;27(5):756-66. doi: 10.1007/s11095-009-0046-5, PMID 20204472.
23. Dewettinck K, Huyghebaert A. Fluidized bed coating in food technology. Trends Food Sci Technol. 1999;10(4-5):163-8. doi: 10.1016/S0924-2244(99)00041-2.
24. Teunou E, Poncelet D. Batch and continuous fluid bed coating review and state of the art. J Food Eng. 2002;53(4):325-40. doi: 10.1016/S0260-8774(01)00173-X.
25. Turk M, Sibanc R, Dreu R, Frankiewicz M, Sznitowska M. Assessment of mini-tablets coating uniformity as a function of fluid bed coater inlet conditions. Pharmaceutics. 2021;13(5):746. doi: 10.3390/pharmaceutics13050746, PMID 34070006.
26. Foppoli A, Cerea M, Palugan L, Zema L, Melocchi A, Maroni A. Evaluation of powder layering vs. spray-coating techniques in the manufacturing of a swellable/erodible pulsatile delivery system. Drug Dev Ind Pharm. 2020;46(8):1230-7. doi: 10.1080/03639045.2020.1788060, PMID 32597251.
27. Dewettinck K, Huyghebaert A. Top-spray fluidized bed coating: effect of process variables on coating efficiency. LWT Food Sci Technol. 1998;31(6):568-75. doi: 10.1006/fstl.1998.0417.
28. Maniyar D, Kadu P, Baig MI. Critical variables affecting the layering method of pelletization. Futur J Pharm Sci. 2023;9(1):68. doi: 10.1186/s43094-023-00522-z.
29. Kim YI, Pradhan R, Paudel BK, Choi JY, Im HT, Kim JO. Preparation and evaluation of enteric-coated delayed-release pellets of duloxetine hydrochloride using a fluidized bed coater. Arch Pharm Res. 2015;38(12):2163-71. doi: 10.1007/s12272-015-0590-y, PMID 26183280.
30. Arora U, Thakkar V, Baldaniya L, Gohel MC. Fabrication and evaluation of fast-disintegrating pellets of cilostazol. Drug Dev Ind Pharm. 2020;46(12):1927-46. doi: 10.1080/03639045.2020.1826509, PMID 33026265.
31. Kumari MH, Samatha K, Balaji A, Shankar MU. Recent novel advandcements in pellet formulation: a review. Int J Pharm Sci Res. 2013;4(10):3803. doi: 10.13040/IJPSR.0975-8232.4(10).3803-22.
32. Gautam N. Wurster based pelletization technique a qualitative approach. Elixir Int J. 2014;74:27131-6.
33. Battu S, Yalavarthi PR, Subba Reddy GV, Uma Maheswara Rao V, Jyothshna Devi K, Vadlamudi HC. Design and assessment of pulsatile technology-based chronomodulated delivery systems of nifedipine. Beni Suef Univ J Basic Appl Sci. 2018;7(4):441-5. doi: 10.1016/j.bjbas.2018.03.012.
34. Balagani PK, Chandiran I, Bhavya B, Sindhuri M. Microparticulate drug delivery system: a review. Indian J Pharm Sci. 2011;1(1):19-37.
35. Mohylyuk V, Patel K, Scott N, Richardson C, Murnane D, Liu F. Wurster fluidised bed coating of microparticles: towards scalable production of oral sustained-release liquid medicines for patients with swallowing difficulties. AAPS PharmSciTech. 2019;21(1):3. doi: 10.1208/s12249-019-1534-5, PMID 31713006.
36. Xu M, Liew CV, Heng PW. Evaluation of the coat quality of sustained release pellets by individual pellet dissolution methodology. Int J Pharm. 2015;478(1):318-27. doi: 10.1016/j.ijpharm.2014.11.057, PMID 25435182.
37. Gryczova E, Dvorackova K, Rabiskova M. Evaluation of pellet friability. Ces Slov Farm. 2009;58(1):9-13.
38. Shafer EG, Wollish EG, Engel CE. The "Roche" Friabilator. Journal of the American Pharmaceutical Association (Scientific ed.). 1956;45(2):114-6. doi: 10.1002/jps.3030450214.
39. Kaur V, Goyal AK, Ghosh G, Chandra Si S, Rath G. Development and characterization of pellets for targeted delivery of 5-fluorouracil and phytic acid for treatment of colon cancer in Wistar rat. Heliyon. 2020;6(1):e03125. doi: 10.1016/j.heliyon.2019.e03125, PMID 32042938.
40. Shah RB, Tawakkul MA, Khan MA. Comparative evaluation of flow for pharmaceutical powders and granules. AAPS PharmSciTech. 2008;9(1):250-8. doi: 10.1208/s12249-008-9046-8, PMID 18446489.
41. Sarraguca MC, Cruz AV, Soares SO, Amaral HR, Costa PC, Lopes JA. Determination of flow properties of pharmaceutical powders by near infrared spectroscopy. J Pharm Biomed Anal. 2010;52(4):484-92. doi: 10.1016/j.jpba.2010.01.038, PMID 20167448.
42. Zhang P, Shadambikar G, Almutairi M, Bandari S, Repka MA. Approaches for developing acyclovir gastro-retentive formulations using hot melt extrusion technology. J Drug Deliv Sci Technol. 2020;60:102002. doi: 10.1016/j.jddst.2020.102002.

43. Dhulipalla Mounika, I Deepika Reddy, K Sai Chandralekha, Kapu Harika, Ramarao Nadendla, Madhu Gudipati. Formulation and *in vitro* evaluation of ciprofloxacin HCL floating matrix tablets. Int J Res Pharm Sci & Tech. 2020;2(1):1-6. doi: 10.33974/ijrpst.v2i1.221.
44. Clinical Pharmacology and Biopharmaceutics Review(S): Addendum to NDA 202-439 for Rivaroxaban (XARELTO®) U.S. Food and Drug Administration. Available from: https://www.accessdata.fda.Gov/drugsatfda_docs/nda/2011/202439orig1s000linpharmr.pdf. [Last accessed on 08 Aug 2025].
45. Celebier M, Kaynak MS, Altinoz S, Sahin S. UV spectrophotometric method for determination of the dissolution profile of rivaroxaban. Diss Technol. 2014;21(4):56-9. doi: 10.14227/DT210414P56.
46. Soni PK, Saini TR. Formulation design and optimization of cationic-charged liposomes of brimonidine tartrate for effective ocular drug delivery by design of experiment (DoE) approach. Drug Dev Ind Pharm. 2021;47(11):1847-66. doi: 10.1080/03639045.2022.2070198, PMID 35484943.
47. Prakash A, Soni PK, Paswan SK, Saini TR. Formulation and optimization of mucoadhesive buccal film for nicotine replacement therapy. Int J App Pharm. 2023;15(3):100-12. doi: 10.22159/ijap.2023v15i3.47412.
48. Costa P, Sousa Lobo JM. Modeling and comparison of dissolution profiles. Eur J Pharm Sci. 2001;13(2):123-33. doi: 10.1016/S0928-0987(01)00095-1, PMID 11297896.
49. Chandwani S, Saini TR, Soni R, Paswan SK, Soni PK. Box-behnken design optimization of salicylic acid loaded liposomal gel formulation for treatment of foot corn. Int J App Pharm. 2023;15(3):220-33. doi: 10.22159/ijap.2023v15i3.47455.
50. Tiwari A, Sharma S, Soni PK, Paswan SK. Fabrication and development of dissolving microneedle patch of butorphanol tartrate. Int J App Pharm. 2023;15(3):261-71. doi: 10.22159/ijap.2023v15i3.47411.
51. Dehariya P, Soni R, Paswan SK, Soni PK. Design of experiment based formulation optimization of chitosan-coated nano-liposomes of progesterone for effective oral delivery. J Appl Pharm Sci. 2023;13(6):256-70. doi: 10.7324/JAPS.2023.142351.
52. Sahoo SK, Jena MK, Dhala S, Barik BB. Formulation and evaluation of gelatin micropellets of aceclofenac: effect of process variables on encapsulation efficiency particle size and drug release. Indian J Pharm Sci. 2008;70(6):795-8. doi: 10.4103/0250-474X.49126, PMID 21369445.
53. Kaffash E, Badiee A, Akhgari A, Akhavan Rezayat NA, Abbaspour M, Saremnejad F. Development and characterization of a multiparticulate drug delivery system containing indomethacin-phospholipid complex to improve dissolution rate. J Drug Deliv Sci Technol. 2019;53:101177. doi: 10.1016/j.jddst.2019.101177.
54. Soni PK, Saini TR. Formulation design and optimization of cationic-charged liposomes of brimonidine tartrate for effective ocular drug delivery by design of experiment (DoE) approach. Drug Dev Ind Pharm. 2021;47(11):1847-66. doi: 10.1080/03639045.2022.2070198, PMID 35484943.
55. Chopra R, Podczeck F, Newton JM, Alderborn G. The influence of pellet shape and film coating on the filling of pellets into hard shell capsules. Eur J Pharm Biopharm. 2002;53(3):327-33. doi: 10.1016/S0939-6411(02)00015-2, PMID 11976021.
56. Dumpala RL, Patil C. A review on pellets and pelletization techniques. Int J Res PharmSci Technol. 2020;2(4):9-21.
57. Zeeshan F, Bukhari NI. Development and evaluation of a novel modified-release pellet-based tablet system for the delivery of loratadine and pseudoephedrine hydrochloride as model drugs. AAPS PharmSciTech. 2010;11(2):910-6. doi: 10.1208/s12249-010-9456-2, PMID 20496016.
58. Nagaraju N, Soni PK, Mukherji G. Water dispersible pharmaceutical formulation and process for preparing the same. Patent no. WO2008104996A2; 2009.
59. Baggi RB, Kilaru NB. Calculation of predominant drug release mechanism using peppas-sahlin model part-i (substitution method): a linear regression approach. Asian J Pharm Technol. 2016;6(4):223-30. doi: 10.5958/2231-5713.2016.00033.7.
60. Yang HS, Kim DW. Fabrication of gastro-floating famotidine tablets: hydroxypropyl methylcellulose-based semisolid extrusion 3D printing. Pharmaceutics. 2023;15(2):316. doi: 10.3390/pharmaceutics15020316, PMID 36839639.